J Solid State Electrochem (2010) 14:1261–1268
DOI 10.1007/s10008-009-0922-2

ORIGINAL PAPER

Voltammetric and conductometric behavior of nanocomposites of polyaniline and gold nanoparticles prepared by layer-by-layer technique

Ulrich Lange · Svetlozar Ivanov · Vladimir Lyutov · Vessela Tsakova · Vladimir M. Mirsky

Received: 6 July 2009 / Revised: 27 July 2009 / Accepted: 11 August 2009 / Published online: 16 September 2009
© Springer-Verlag 2009

Abstract Multilayer nanocomposites from polyaniline (PANI) and gold nanoparticles (AuNPs) were formed by layer-by-layer deposition. The formation of PANI–AuNPs multilayer structures was monitored by UV-vis absorption spectroscopy and cyclic voltammetry. Each deposited bilayer of PANI–AuNPs led to a monotonous and almost linear increase in both optical absorbance and the first current peak of PANI oxidation. The prepared multilayer nanocomposites were characterized by in situ conductivity measurements at different pH and potential and by transmission electron microscopy. Finally, chemosensitive properties of the new material based on the intrinsic affinity of gold nanoparticles were studied. Changes in the film resistance on exposure to vapors of mercury and sulfur-containing compounds were observed.

Keywords Polyaniline · Gold nanoparticles · Layer-by-layer deposition · Chemoresistor · In situ conductivity measurements · Nanocomposite

U. Lange · V. M. Mirsky
Institute of Analytical Chemistry, Chemo- and Biosensors, University of Regensburg, 93047 Regensburg, Germany

S. Ivanov · V. Lyutov · V. Tsakova
Institute of Physical Chemistry, Bulgarian Academy of Sciences, 1113 Sofia, Bulgaria

V. M. Mirsky (✉)
Department of Nanobiotechnology, Lausitz University of Applied Sciences, 01968 Senftenberg, Germany
e-mail: vmirsky@hs-lausitz.de

Introduction

The layer-by-layer (LbL) deposition based on interactions between polyions with alternating charges first introduced by Decher et al. [1–3] offers a simple procedure for formation of multilayered structures. Since the early works of Rubner et al. [4–6], this approach has been explored extensively for deposition of different conducting polymers. Due to the easy processability (noncomplicated chemical synthesis and solubility in slightly acidic aqueous media), polyaniline belongs to the most studied conducting polymers in these investigations. Various species, i.e., polyanions [5,7], polycations [6,8,9], semiconductor particles [10–14], nonionic soluble polymers [15], and, more recently, metal complexes [16–18], proteins [19–21], enzymes [22], and carbon nanotubes [23] were used in combination with PANI, sulfonated PANI [7,13,19–22], or other polyaniline derivatives [7].

PANI gold composites have been formed by electrochemical deposition of gold in PANI [24] or by reduction of tetrachloroaurate [24,25] or tetrabromoaurate [26] by PANI. Recently, the layer-by-layer technique was applied to form composites of PANI and anion-coated AuNPs [27–29]. The interest into incorporation of anion-coated metal nanoparticles in PANI is based on the following two reasons: (1) incorporation of metallic electrocatalytic centers into the polymer structure and (2) doping of PANI with immobilized anionic component and thus, shifting the pH range of PANI electroactivity towards the practically important range of neutral pH. A further point of interest is a possible application of gold PANI nanocomposites as a chemosensitive material [30].

In this work, we studied multilayered PANI–AuNP nanocomposites using gold nanoparticles synthesized according to the technique of Turkevich [31] that is based

on the reduction of $AuCl_4^-$ in citrate medium. A high affinity of gold to mercury (0) and sulfuric compounds is well known and is used actively for the development of chemosensors [32–34]. In the case of a close contact of PANI and AuNPs, the interaction of gold with these compounds may affect the electrochemical and conductive properties of the PANI–AuNP nanocomposite. To achieve this interaction, the nanoparticles should be either uncoated or coated by a weakly adsorbed monomolecular layer. This was the reason to focus on a composite material prepared by using gold nanoparticles without further modification or with just a dialysis treatment. According to our knowledge, this is the first combined investigation of electrochemical, spectroscopical, and in situ conductivity properties of an LbL-deposited composite material of this type.

Experimental

PANI was synthesized by chemical oxidative polymerization in the presence of 0.1 M aniline, 0.1 M ammonium persulfate, and 0.5 M sulfuric acid for 6 h at 4 °C under continuous stirring. The polyaniline, synthesized as emeraldine salt, was transformed to emeraldine base by treating with ammonia. According to the procedure of Rubner et al. [4], the obtained product was washed and dissolved in dimethylacetamide (20 mg dried emeraldine base per ml) under continuous stirring and subsequent sonication. After filtering with Millipore filter (0.5 μm), the solution was diluted ten or 100 times using diluted HCl (pH 3.1). Finally, the pH of the PANI-containing solution was adjusted to pH 2.6. Electropolymerization of PANI–citrate on an Indium Tin Oxide (ITO)-covered glass electrode was done from a solution containing 0.1 M citric acid and 0.05 M aniline at 0.9 V vs Saturated Calomel Electrode (SCE). The charge was 10 mC/cm^2.

The AuNP solution was prepared by fast injection of 500 μl of 2 % (*w*/*w*) sodium citrate in water to 10 ml of a boiling solution of 1 mM $HAuCl_4$ under rapid stirring. Stirring was continued until the typical red coloration of the mixture appeared and was followed by cooling down to room temperature. The excess of citrate was removed by diafiltration using a Masterflex tangential flow filtration system (www.pall.com) with a membrane (Omega 10 K Membrane, Minimate TFF Capsule, www.pall.com) keeping the volume of the AuNP solution constant by addition of Millipore water. The suspension was stable within few months thus indicating that a rest amount of citrate remains on the gold surface and contributes into its surface charge. The negative values of *z*-potential were also confirmed by measurements of dynamic light scattering using z-Sizer Nano-ZS Malvern (www.malvern.com). The LbL self assembly was started by dipping the gold or ITO glass electrode for 20 min first in PANI and then in AuNP solutions. For the next bilayers, the duration of the adsorption steps was fixed to 10 min. After each PANI adsorption step, the electrode was washed in HCl aqueous solution (pH 2.6). For comparison, LbL self-assembled layers were also obtained by using 1 mM poly(sodium styrene sulfonate; PSS) instead of AuNP solution. An adsorption of PANI onto gold surface was also confirmed by surface plasmon resonance technique using SPR spectrometer Biosuplar-410 (www.biosuplar.com). The adsorption of the first PANI layer on ITO was confirmed by cyclic voltammetry in 0.5 M H_2SO_4 (Fig. 1). In general, physical adsorption of polymers to many surfaces can be enhanced by interaction of polymer charges with induced charges in the conducting substrate. The subsequent adsorption of PANI and AuNPs or PSS is based on electrostatic attraction between oppositely charged species.

All electrochemical measurements were carried out with Autolab PGSTAT-12 (www.ecochemie.nl) in a three-electrode configuration. ITO glasses with surface area of 1.5 cm^2 or metal interdigitated electrodes were used as working electrodes; platinum plates served as counter electrodes. SCE reference electrodes were used in the voltammetric investigations, and all potentials in the text, including spectroelectrochemical data, are referred to this reference electrode. The experiments were performed at room temperature (20 °C).

Investigations of the pH dependence of the electrochemical activity and conductance of the multilayer PANI-based structures were carried out in buffer solutions with the following compositions: (1) 0.1 M NaCl+10 mM NaH_2PO_4/H_3PO_4 for pH range from 2 to 3; (2) 0.1 M NaCl+10 mM CH_3COOH/CH_3COONa for pH range from 4 to 5; (3) 0.1 M NaCl+10 mM Na_2HPO_4/NaH_2PO_4 for pH range from 6 to 7. Deionized water additionally purified by Millipore Milli Q system was used for the preparation of all solutions.

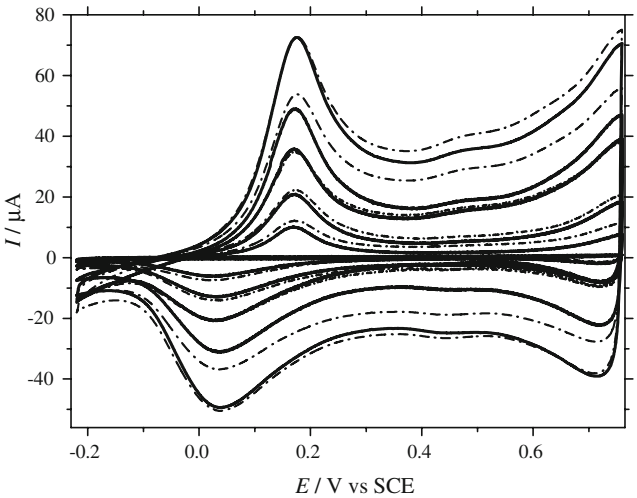

Fig. 1 Voltammetric curves measured in 0.5 M H_2SO_4 for the first five bilayers of PANI–AuNPs after every PANI (*solid line*) and AuNPs (*dotted line*) deposition step

TEM imaging was carried out using JEOL JEM 100 B transmission electron microscope. The specimens for TEM were prepared by casting the AuNPs from solution or by LbL self-assembly directly on Formvar®-coated Au mesh for TEM. Ultraviolet-visible (UV-vis) absorption spectroscopy and spectroelectrochemical measurements were performed using a Cary 50Bio spectrophotometer from Varian in a 1-cm cell. A two-electrode configuration with Ag/AgCl electrode was used for spectroelectrochemical measurements. Interdigitated thin platinum or gold electrodes on oxide-coated silicon supports were used for 2- and 4-point conductivity measurements. They consist of four parallel metallic strips with the width of 10 μm (outer strips) and 5 μm (inner strips) with a 5-μm gap between each strip. The strips are repeatedly folded to fit a square spot of 500 x 500 μm [35–37]. The electrodes designed for two-point measurements only have similar geometry, but without two inner electrodes, the gap between electrodes was 10 μm. Thus, the whole macroscopic electrode area including the gaps between the conducting strips was about 2.5 10^{-3} cm^2. The electrodes were cleaned before the experiments with a hot "piranha" solution consisting of a freshly prepared mixture of 30% hydrogen peroxide and 96% sulfuric acid (1:3, *v*/*v*). Caution: piranha solution reacts violently with many organic materials and must be handled with extreme care. Simultaneous two- and four-point conductivity measurements were carried out by applying potential pulses of 50 mV with alternating polarity between the outer strips and measuring the current through the outer and the voltage between the inner strips. The measurement system was controlled by HP Vee software. A detailed description of the measurement technique can be found in [35–37]. The conductivity measurements were carried out at controlled electrical potential of the interdigitated electrode relative to SCE. Two-point measurements were applied for investigation of the response to different vapors. The electrodes were covered by ten bilayers of the AuNP-PANI nanocomposite. In the investigation of the conductometric response towards octanthiol and dimethyldisulfide, the composite was deprotonated in a pH 7 buffer and dried before measurements. To measure the response towards octanthiol and dimethyldisulfide, 10 mL of the headspace of these compounds was passed through a 2-mL flow cell in which the sample was placed. For investigations of the response towards mercury, the nanocomposite was protonated by pretreatment at pH 2.6 and dried. Then, a small droplet of mercury was placed in the sealed measurement chamber with a 1-μL pipette.

Results and discussion

TEM characterization and UV-vis absorption spectroscopy

PANI–AuNPs coatings consisting of three bilayers were used for TEM imaging (Fig. 2). The size of the gold nanoparticles immobilized in the LbL structure varies between 20–40 nm. The image indicates that the individual nanoparticles are coated by a shell, which is not the case for AuNPs directly cast on a TEM mesh without PANI. Assuming that the surface properties of Formvar®-coated by PANI are similar to that of gold and ITO electrodes coated by PANI, one can make a course estimation of surface density of AuNPs on the electrodes from the analysis of TEM images. The particle density in the TEM images is about 4.2 10^{10} particles per cm^2; the total area coated by nanoparticles after deposition of three bilayers is estimated from the micrograph to be about 26 %.

The subsequent adsorption of four PANI–AuNPs bilayers was monitored by absorption spectroscopy showing an increase in the absorbance signal (Fig. 3a). These measurements were carried out in air after rinsing the LbL-deposited PANI–AuNPs structures with diluted HCl solution at pH 2.6. The absorption spectra are composed of at least two absorbance bands, the first one being the gold plasmonic band with absorption maximum at about 520 nm

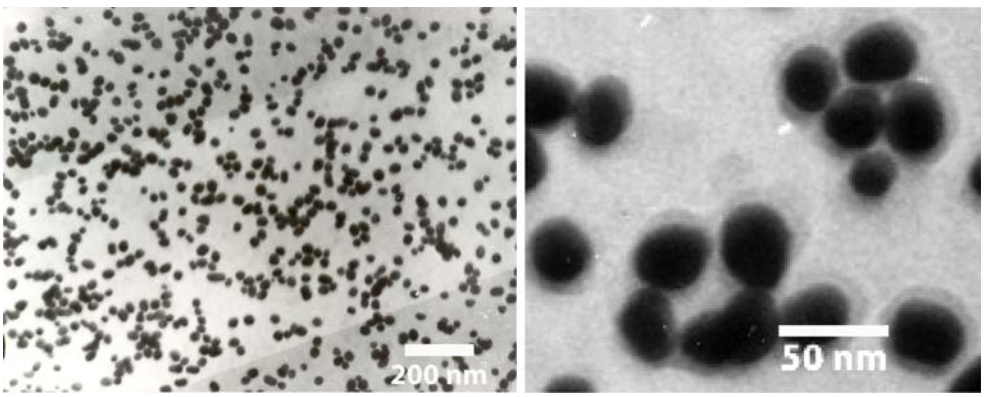

Fig. 2 TEM images of the nanocomposite consisting of three bilayers of AuNPs and PANI at different magnifications

[38] which overlaps the second absorbance band with a maximum at about 625 nm. A comparison between the spectra of AuNPs in solution, LbL-assembled PANI–AuNPs, and electropolymerized PANI–citrate is presented in Fig. 3b. It is evident that the second absorption peak observed in the PANI–AuNPs case could be attributed neither to noninteracting AuNPs (a sharp single maximum at about 520 nm is observed in this case) nor to doped PANI—a large absorbance band starts emerging for much longer wavelengths. The deconvolution of the absorbance peaks (Fig. 3a) shows that the ratio of the absorbance within the two observed bands is changing with number of deposited bilayers, the second absorbance band becoming dominant after the deposition of the second bilayer. On the other hand, the deconvoluted short wavelength absorption peak shifts gradually from 520 nm (equivalent to the absorption of AuNPs dissolved in solution) to about 550 nm. A bathochromic shift in the AuNPs gold plasmonic band can result from the variation of the refractive index of the AuNPs environment [39]. A gradual shift in the gold plasmonic peak was already observed when increasing the number of polyelectrolyte layers deposited over initially adsorbed AuNPs [40].

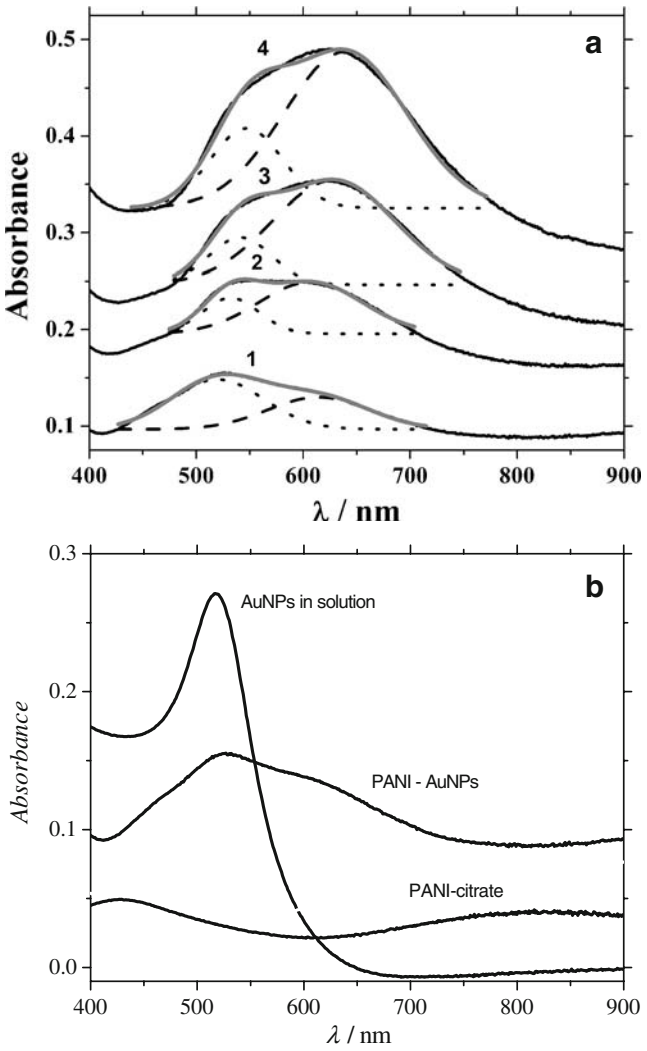

Fig. 3 Absorption spectra obtained for deposition of four subsequent bilayers of PANI–AuNPs (**a**) and a comparison between absorbance spectra of PANI–AuNPs, PANI–citrate, and freshly synthesized AuNPs (**b**). The measurements of the PANI–AuNPs nanocomposite and of PANI–citrate were performed in air. The number in the panel (a) corresponds to the number of the deposited bilayers. Deconvolution of the adsorption peaks is indicated by interrupted lines

The appearance and growth of the second long wavelength absorbance band could be possibly attributed to collective resonance of the AuNPs with increasing density in the course of the LbL deposition. Double-band absorbance spectra have been already found in the systems AuNPs-poly (ethylene imine) [40] and AuNPs-poly(allylaminehydrochloride)-PSS [41] deposited as supported layers. By gradually increasing the Au coverage, the emerging of a second absorption band at about 620 nm (coexisting with the normal plasmonic band at 520 nm) was found [41]. The second peak was attributed to the collective plasmon resonance of AuNPs. It was suggested that the collective surface plasmon band depends strongly on the interparticle separation. This effect was observed for LbL deposited AuNPs [41] the LbL procedure providing close intra- in interlayer AuNPs interactions. On the other hand, investigations on the absorbance of Au-PANI colloid solutions obtained through one-pot chemical synthesis of the Au-PANI composite show a quite different behavior [42–44]. A strong suppression of the gold plasmonic peak was observed and interpreted as due to AuNPs–PANI interaction. A similar effect was reported for coating of gold nanoparticles with a relatively thick (100 nm) layer of PANI [45]. In these cases, however, gold and PANI are supposed to be in direct contact and may interact in a very different way in comparison to the anion-stabilized presynthesized AuNPs which are introduced into PANI through electrostatic interactions. It is interesting to note that the one-pot synthesis of AuNPs-modified-PANI (i.e., poly-3-aminophenylboronic acid) in the presence of a stabilizer (poly-vinyl alcohol) allows keeping the gold plasmonic peak in the absorbance spectrum [46]. A second absorption peak at longer wavelength does not appear probably due to the large interparticle distances and the lack of the collective resonance.

The electrochromic properties of the PANI–AuNPs nanocomposite were studied by in situ spectroelectrochemical measurements performed on an ITO electrode covered with four PANI–AuNPs bilayers. The measurements were carried out in acidic solution (0.5 M H_2SO_4) which means that PANI was additionally doped and thus, in a higher oxidation state. The absorbance spectra (Fig. 4) show the appearance of a single band (around 550 nm) that corresponds to the position of the deconvoluted gold plasmonic peak for the 4-bilayers structure (Fig. 3). The second absorbance band disappears

from the absorbance spectra thus indicating disturbance of the collective resonance of AuNPs. This may be caused by polymer swelling in solution or by different extent of PANI doping (at pH 2.7 and pH≈0, correspondingly) which, in turn, affects the conductivity of PANI and also the PANI chains conformation and thus, finally, the AuNPs interparticle distance. A decrease of the plasmon absorbance band was observed with increasing potential (from −0.1 V to 0.7 V) and also a small hypsochromic shift and broadening of the absorbance peak. At a higher potential (0.9 V, gray line), the absorbance increases again. A much stronger shift of the absorbance band was observed depending on the oxidation state of PANI when covering gold nanoparticles with a 100-nm thick PANI layer [45]. The absorbance peaks for the two states of PANI were resolved by more than 60 nm, and the peak was strongly suppressed in the case of oxidized PANI. This result suggests that the interaction between PANI and AuNPs depends on the specific surroundings of the AuNPs, and it becomes more pronounced for the oxidized, high-conducting state of PANI. Thus, the shift of the plasmonic band with potential observed in our investigation should be due to the influence of oxidized PANI on the resonance of plasmons. To estimate this effect, the shift of the peak position and of the maximal absorbance was simulated using Mie equation [47], and the data [48] on real and imaginary components of the refractive index of gold. It was found that the observed electrochemically driven hypsochromic shift of the plasmonic absorption peak corresponds to a decrease of the refractive index of PANI by 0.07. A similar observation of electrochemical control of the plasmonic absorption peak was reported earlier for AuNPs deposited between two layers of electropolymerized PANI [49]. It was suggested that the modification of the plasmonic absorbance band relates to changes of the real and imaginary parts of the dielectric constant of PANI. Such changes of the dielectric constants were measured directly [50] by means of surface plasmon resonance spectroscopy in Kretschmann configuration.

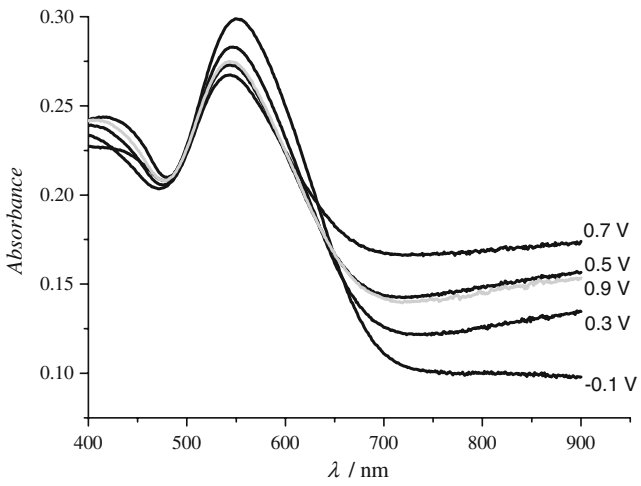

Fig. 4 Absorption spectra of four bilayers of PANI–AuNPs measured at different potentials in 0.5 M sulfuric acid

Cyclic voltammetry

Figure 1 presents cyclic voltammetric curves measured in 0.5 M H_2SO_4 after adsorption of each subsequent PANI or AuNPs layer. The potentiodynamic curves demonstrate the usual oxidation behavior of polyaniline, i.e., the leucoemeraldine to emeraldine (first anodic peak) and emeraldine to pernigraniline (peak starting at 0.6 V) oxidations and the corresponding reverse reduction processes. The appearance of hydrogen reduction currents close to the negative potential scan limit gives an evidence for the electrocatalytic activity of the gold nanopartcles immobilized in the LbL structure.

It is interesting to note the increase in the electrochemical activity of PANI after each AuNPs adsorption step (*dotted lines*). This effect could be attributed to additional chemical doping of the polymer by the adsorbed AuNPs. A similar conclusion was made by Zou et al. [29] for PANI–mercaptoethane sulfonate-stabilized AuNPs and AgNPs based on comparative UV-vis near-IR investigations of the LbL-assembled PANI structures. The authors suggest that AuNPs and AgNPs provide more effective doping of PANI and improve its conductivity.

Figure 5 shows the dependence of the oxidation charge of the multilayered composite structure calculated from the cyclic voltammograms on the number of deposited bilayers. Dialyzed and nondialyzed AuNPs solutions were used for the AuNPs adsorption step. The comparison shows a stronger increase in Q_{ox} in the case of nondialyzed AuNPs solution probably due to the higher amount of citrate adsorbed on the Au particles surface. This should result in enhancement of the negative surface charge of the AuNPs, which makes the interaction between the positively charged PANI chains and AuNPs more efficient. Another possible reason for the charge increase could be some additional doping of PANI by the excess of citrate ions available in the nondialyzed AuNPs containing solution. In order to estimate the influence of the citrate ions on the electrochemical activity of PANI, a polymer layer deposited in a single adsorption step of PANI alone was first measured by cyclic voltammetry in sulfuric acid and subsequently dipped for 10 min into a citrate-containing solution with the same anion concentration as used for the AuNPs synthesis. Potentiodynamic measurement carried out in sulfuric acid after this treatment showed higher redox charges. Therefore, citrate anions both nonadsorbed and adsorbed on AuNPs should be involved in the PANI layer doping in the course of the AuNPs deposition steps. A good

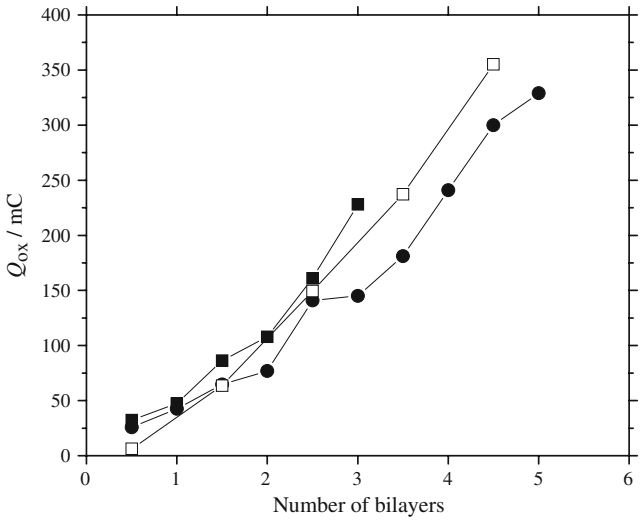

Fig. 5 Dependences of Q_{ox} on the number (n) of deposite bilayers of PANI–AuNPs for dialyzed (*squares*) and nondialyzed (*circles*) gold nanoparticles. The data obtained after deposition of AuNPs correspond to whole numbers of bilayer; the points in between correspond to the data obtained after deposition of PANI. The *filled* and *open squares* indicate the data from two separate LbL runs

reproducibility of the LbL procedure for building PANI–AuNPs structures is demonstrated for two separate LbL deposition runs (Fig. 5).

Further voltammetric experiments were carried out in buffer solutions with different acidity (pH from 1 to 7; Fig. 6). The measurements show well-pronounced electrochemical activity of the LbL-deposited layers in the pH range 1–6. With increasing pH, the two intrinsic PANI redox couples gradually shift together, and finally, at pH 5 and 6, single broad oxidation and reduction peaks are observed. Between pH 6 and 7, the LbL-assembled PANI structure loses, almost completely, its electrochemical activity probably due to the transformation from emeraldine-salt to emeraldine-base. Similar observations were made for LbL-assembled PANI–AuNPs stabilized with mercaptosuccinic acid [28]. The authors report for appreciable electrochemical activity of PANI at pH values as high as pH 8. However, in this case [28], the measurements were carried out in citrate–phosphate buffers, the citrate anions having possibly an additional doping effect on PANI. It was shown that conventional PANI (i.e., PANI doped with small inorganic anions) shows electroactivity in the presence of citrate anions [51].

Conductance measurements

The "in situ" conductance of a PANI–AuNPs LbL structure consisting of ten bilayers was investigated at different fixed potentials in buffer solutions at pH 2–7 (Fig. 7). The PANI–AuNPs nanocomposite loses gradually its conductivity with increasing pH. Also, the potential window corresponding to the high conductivity state of PANI becomes narrower. This is in accordance with the shift of the emeraldine to the pernigraniline oxidation peaks observed in the voltammetric experiments.

The data on the conductance of the PANI–AuNPs nanocomposite multilayer were compared with data obtained on PANI/PSS LbL-deposited films (Fig. 8). The conductances were normalized to the electrochemical oxidation charge obtained from the voltammetric measurements in 0.5 M H_2SO_4 solution. Notably, at pH 2, the LbL-deposited PANI–AuNPs structure shows a lower conductivity in the reduced (leucoemeraldine) state in comparison with the PANI–PSS system. At pH 6, the PANI–AuNPs layers also have lower conductance in comparison with the PANI–PSS LbL

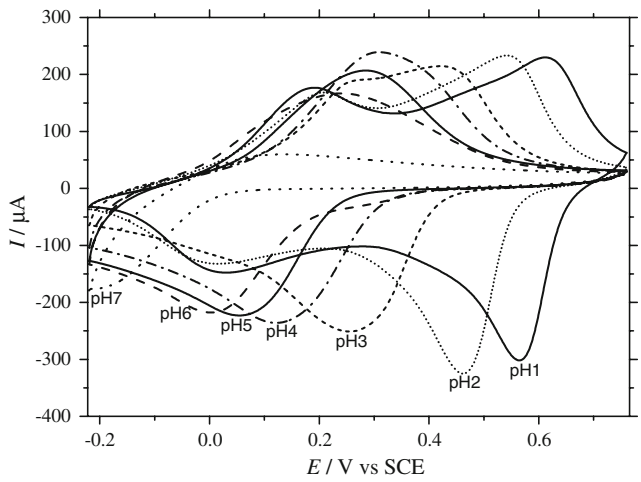

Fig. 6 Voltammetric curves of PANI–AuNPs nanocomposite consisting of ten bilayers measured in buffer solutions at different pH

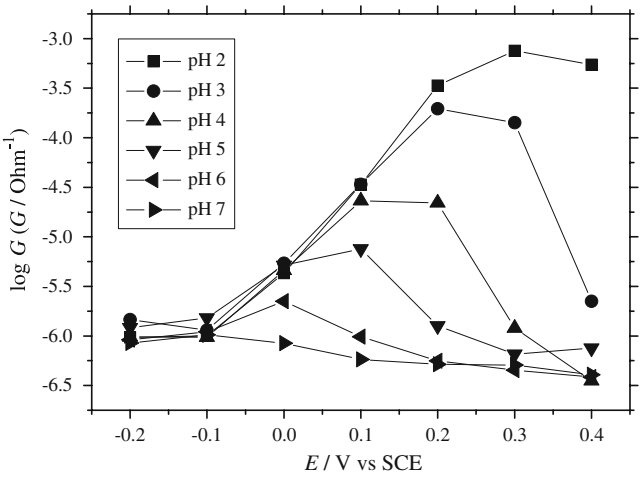

Fig. 7 Potential dependence of conductance of PANI–AuNPs nanocomposite consisting of ten bilayers measured in buffer solutions at different pH

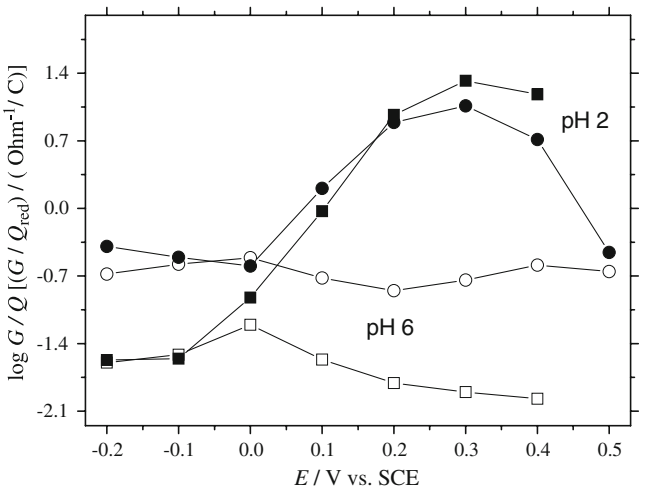

Fig. 8 Potential dependence of conductance of PANI–AuNPs (*squares*) and PANI–PSS (*circles*) measured at two different pHs

structures (Fig. 8). The difference in the conductance in the reduced state could be related to various factors, e.g., a higher ionic conductivity in the case of PANI–PSS layers, provided by the PSS anions or a possible structural difference between both types of LbL multilayers. In comparison to PANI–AuNPs, the PANI–PSS structure may be more ordered and uniform due to the template-like influence of the adsorbed PSS.

Conductommetric response in the presence of different analytes

The gold surface has a high affinity to mercury vapor and to some sulfuric compounds (thiols, disulfides). Therefore, one can expect that the gold nanoparticles incorporated in the PANI–AuNPs nanocomposites bind these compounds resulting in a modification of the physical properties of the composite material. The conductometric response of the nanocomposite multilayer structures to vapors of mercury, octanthiol, and dimethyldisulfide were measured. Figure 9 (left) shows the response of a deprotonated PANI–AuNPs LbL-coated interdigitated electrode on injection of 10 mL of the headspace of octanthiol and dimethyldisulfide performed in a 2-mL flow cell. The observed drop in resistance was specific for the PANI–AuNPs nanocomposite multilayer and was not found for the electrodes coated by PANI/PSS multilayer films. Therefore, the binding of these compounds to the gold nanoparticles is responsible for the resistance decrease. The stronger decrease of the resistance in case of dimethyldisulfide (about 50 times decrease in comparison to 6.5 times decrease) can be explained by a higher vapor pressure of this compound in comparison with octanthiol. A similar behavior was found on exposure of the protonated form of the nanocomposite to mercury vapor (Fig. 9, right). Again, this effect was not observed for PANI/PSS films. In the cases of thiol and disulfide, the resistance decrease of the layers might be explained by release of dopants from the AuNP shell in the PANI upon binding of the thiols/disulfides. In the case of mercury vapor, an explanation is more difficult and may include changes of the affinity of citrate to the metallic surface after amalgam formation. Both effects are irreversible upon exposure of the sample to air; this complicates an investigation of concentration dependencies. Although the physical and chemical mechanisms of the observed effect are not clear, it is to note that the effects are the consequence of the modification of PANI by gold nanoparticles. One can expect further development of this approach by deposition of selectively permeable monomolecular layers [33] or by deposition of nanoparticles with immobilized receptors.

Conclusions

This study demonstrates the possibility to obtain multilayered structures of PANI and AuNPs. The proposed LbL approach results in the formation of PANI shells around AuNPs that prevents their further agglomeration. The protective shell does

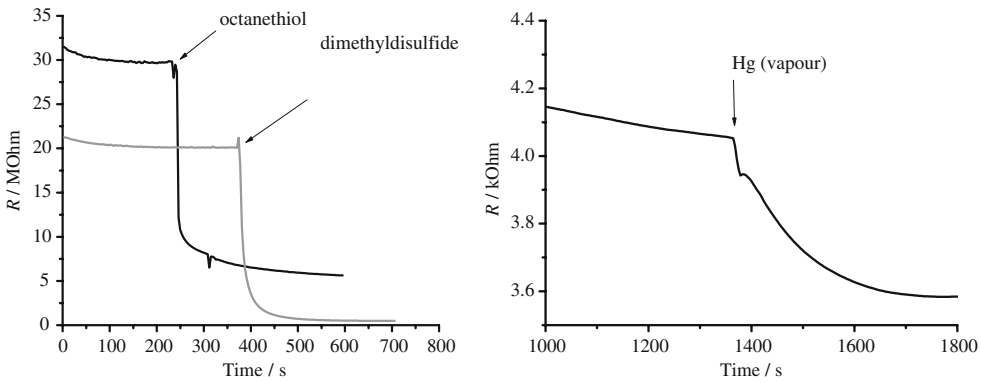

Fig. 9 Conductometric response of a nanocomposite consisting of ten bilayers of PANI–AuNPs on exposure to octanethiol and dimethyldisulfide (*left*) and mercury (*right*) vapors

not impede the electrochemical activity of AuNPs in the nanocomposite. In the same time, the citrate anions introduced into the multilayer structure through the AuNPs adsorption steps provide a stable doping of the PANI structure resulting in an appreciable electroactivity and conductivity at close to neutral pH values. The spectroelectrochemical measurements of the PANI–AuNPs nanocomposite show that the physical properties of this nanocomposite multilayer structure cannot be described as a superposition of properties of both components but result from the interaction of AuNPs and the polymer.

The sensitivity of the resistance of the synthesized PANI–AuNPs nanocomposite on exposure to compounds with high affinity to gold gave evidence for their binding to the Au surface. Although it is difficult to make exact predictions on the perspective applications of this system at the present stage of investigation, one can suggest further improvement of these properties by immobilization of receptors on the surface of the nanoparticles. The incorporation of metal nanoparticles with preimmobilized receptors into conducting polymers could be a general technology for the formation of chemosensitive materials with a wide spectrum of selectivity and affinity. The LbL deposition of polymer–nanoparticle multilayer structures can be also performed in flow mode and combined with combinatorial approaches for further optimization of their chemosensitive properties [52,53].

Acknowledgements The investigations are completed in the frameworks of the bilateral contract PPP Bulgarien–DAAD-07/2007 supported by DAAD and Bulgarian Ministry of Education and Science and the contracts VUH307/2007 and SP 40/2008 supported by Bulgarian Ministry of Education and Science. U. L. was supported by DFG (GRK 640; Sensory photoreceptors in natural and artificial systems). The authors are grateful to Dr. V. Kulikov and L. Spektor for the development of software for the measurement system.

References

1. Decher G (1997) Science 277:1232
2. Lvov Y, Decher G, Moehwald H (1993) Langmuir 9:481
3. Decher G, Lvov Y, Schmitt J (1994) Thin Solid Films 244:772
4. Ferreira M, Cheung J, Rubner M (1994) Thin Solid Films 244:806
5. Cheung J, Fou A, Rubner M (1994) Thin Solid Films 244:985
6. Ferreira M, Rubner M (1995) Macromolecules 28:7107
7. Mattoso L, Zucolotto V, Patterno L, van Griethuijsen R, Ferreira M, Campana S, Oliveira O (1995) Synth Met 71:2037
8. Sarkar N, Ram M, Sarkar A, Narizzano R, Paddeu S, Nicolini C (2000) Nanotechnology 11:30
9. Jung S, Kim H, Han M, Kang Y, Kim E (2004) Mat Sci Eng C 24:57
10. Kovtyukhova N, Ollivier PJ, Chizhik S, Dubravin A, Buzaneva E, Gorchinskiy A, Marchenko A, Smirnova N (1999) Thin Solid Films 337:166
11. Kovtyukhova NI, Gorchinskiy A, Waraksa C (2000) Mat Sci Eng B 69–70:424
12. Kovtyukhova NI, Martin BR, Mbindyo JKN, Mallouk TE, Cabassi M, Mayer TS (2002) Mat Sci Eng C 19:255
13. Ma X, Lu G, Yang B (2002) Appl Surf Sci 187:235
14. Huguenin F, Ferreira M, Zucolotto V, Nart FC, Torresi RM, Oliveira ON Jr (2004) Chem Mater 16:2293
15. Stockton W, Rubner M (1997) Macromolecules 30:2717
16. Wang Y, Guo C, Chen Y, Hu C, Yu W (2003) J Colloid Interface Sci 264:176
17. Man KYK, Wong HL, Chan WK, Djurisic AB, Beach E, Rozeveld S (2006) Langmuir 22:3368
18. Zucolotto V, Ferreira M, Cordeiro MR, Constantino CJL, Moreira WC, Oliveira ON Jr (2006) Sens Actuators B 113:809
19. Dronov R, Kurth D, Mohwald H, Scheller F, Lisdat F (2007) Electrochim Acta 53:1107
20. Dronov R, Kurth D, Mohwald H, Scheller F, Friedmann J, Pum D, Sleytr U, Lisdat F (2008) Langmuir 24:8779
21. Spricigo R, Dronov R, Rajagopalan K, Lisdat F, Leimkuehler S, Scheller F, Wollenberger U (2008) Soft Matter 4:972
22. Yu X, Sotzing GA, Papadimitrakopoulos F, Rusling JF (2003) Anal Chem 75:4565
23. Loh KJ, Lynch JP, Kotov NA (2008) Smart Structures and Systems 4:531
24. Kinyanjui JM, Hanks J, Hatchett DW, Smith JA, Josowicz M (2004) J Electrochem Soc 151:D113
25. Sheffer M, Mandler D (2009) Electrochim Acta 54:2951
26. Smith JA, Josowicz M, Janata J (2003) J Electrochem Soc 150: E384
27. Tian S, Liu J, Zhu T, Knoll W (2003) Chem Commun 21:2738
28. Tian S, Liu J, Zhu T, Knoll W (2004) Chem Mater 16:4103
29. Zou X, Bao H, Guo H, Zhang L, Qi L, Jiang J, Niu L, Dong S (2006) J Coll Interf Sci 295:401
30. Hattched DW, Josowicz M (2008) Chem Rev 108:746
31. Turkevitch J, Stevenson PC, Hillier J (1951) Discuss Faraday Soc 11:55
32. McNerney JJ, Buseck PR, Hanson RC (1972) Science 178:611
33. Mirsky VM, Vasjari M, Novotny I, Rehacek V, Tvarozek V, Wolfbeis OS (2002) Nanotechnology 13:175
34. Vasjari M, Mirsky VM (2007) In: Alegret S, Merkoci A (eds.) Electrochemical sensor analysis, Comprehensive analytical chemistry, vol. 49. Elsevier, Amsterdam, pp 1065
35. Hao Q, Kulikov V, Mirsky VM (2003) Sens Actuators B 94:352
36. Kulikov V, Mirsky VM, Delaney T, Donoval D, Koch AW, Wolfbeis OS (2005) Meas Sci Technol 16:95
37. Lange U, Mirsky VM (2008) J Electroanal Chem 622:246
38. Daniel M-C, Astruc D (2004) Chem Rev 104:293
39. Templeton AC, Pietron JJ, Murray RW, Mulvaney PJ (2000) Phys Chem B 104:564
40. Schmitt J, Machtle P, Eck D (1998) Langmuir 15:3256
41. Jiang C, Markutsya S, Tsukruk V (2004) Langmuir 20:882
42. Kinyanjui JM, Hatchett DW, Smith JA, Josowicz M (2004) Chem Mater 16:3390
43. Peng Z, Guo L, Zang Z, Tesche B, Wilke T, Ogermann D, Hu S, Kleinermanns K (2006) Langmuir 22:10915
44. Guo L, Peng Z (2008) Langmuir 24:8971
45. Leroux YR, Lacroix JC, Chane-Ching KI, Fave C, Felidj N, Levi G, Aubard J, Krenn JR, Hohenau A (2005) J Am Chem Soc 127:16022
46. Ma Y, Li N, Yang C, Yang X (2005) Colloids Surf A Physicochem Eng 269:1
47. Mie G (1908) Annalen der Physik 330:377
48. Schulz LG, Tangherlini FR (1954) J Opt Soc Am 44:362
49. Leroux Y, Eang E, Fave C, Trippe G, Lacroix JC (2007) Electrochem Comm 9:1258
50. Baba A, Tian S, Stefano F, Xia C, Wang Z, Advincula RC, Johannsmann D, Knoll W (2004) J Electroanal Chem 562:95
51. Ivanov S, Tsakova V (2002) J Appl Electrochem 32:701
52. Potyrailo RA, Mirsky VM (2008) Chem Rev 108:770
53. Potyrailo RA, Mirsky VM (2007) Combinatorial methods for sensor materials. Springer, New York